Constituent quark model for nuclear stopping in high energy nuclear collisions

T. K. Choi, M. Maruyama, and F. Takagi
Department of Physics, Tohoku University, Sendai, 980-77, Japan
(Received 2 August 1996)

We study nuclear stopping in high energy nuclear collisions using the constituent quark model. It is assumed that wounded nucleons with a different number of interacted quarks hadronize in different ways. The probabilities of having such wounded nucleons are evaluated for proton-proton, proton-nucleus, and nucleus-nucleus collisions. After examining our model in proton-proton and proton-nucleus collisions and fixing the hadronization functions, it is extended to nucleus-nucleus collisions. It is used to calculate the rapidity distribution and the rapidity shift of final-state protons in nucleus-nucleus collisions. The computed results are in good agreement with the experimental data on $^{32}S+^{32}S$ at $E_{lab}=200A$ GeV and $^{208}Pb+^{208}Pb$ at $E_{lab}=160A$ GeV. Theoretical predictions are also given for proton rapidity distribution in $^{197}Au+^{197}Au$ at $\sqrt{s}=200A$ GeV (BNL-RHIC). We predict that the nearly baryon-free region will appear in the midrapidity region and the rapidity shift is $\langle \Delta y \rangle = 2.24$.

PACSnumber(s): 25.75.−q,12.39.−x,13.85.−t,25.40.Ep

I. INTRODUCTION

Whether the incident nucleons are stopped in or pass through the target nucleus is a fundamental and important concern in high energy heavy ion collisions. These two different situations emerge according to collision energy and atomic mass of the nucleus. They suggest different relevant dynamics, the dynamics of shock formation and Landau hydrodynamics [1] in the case of the stopping regime, or the Bjorken longitudinal expansion and inside-outside cascade dynamics [2] in the case of the baryon-free regime. The distinction between the two situations is related to how the incident nucleons slow down by multiple collision with nucleons of the other nucleus and how the collision energy is deposited for particle production. The relevant measure, the nuclear stopping power, provides an estimation of the energy density achieved in collisions. Experimental data indicate so far a baryon-rich regime at midrapidity for a heavy nucleus collision such as gold on gold at AGS energies [3] and sulphur on sulphur [4] or lead on lead [5] at SPS, where the achievement of initial condition for QGP formation is still controversial. The clear baryon-free regime may be realized at RHIC energy region.

For a description of high energy nucleus collision dynamics, there are many theoretical models, which differ in their assumptions as to how the particles share the incident energies, where the sources of particle production are, and how the produced particles hadronize, while having almost the same picture for a multiple collision process of constituents such as the Glauber model [6]. A detailed comparison of these models can be found in Ref. [7] by Werner and Ref. [8] by Wong. In particular, for the proton rapidity density distribution, which is related to how high baryon densities may be attained in reactions, these model predictions show notable difference due to their different assumptions. For example, as discussed by Gyulassy [9], the RQMD [10] predicts a much higher degree of baryon stopping than VENUS [7] and HIJING [11], which predict a concavity at midrapidity for a reaction such as lead on lead collision at SPS energies. In some approaches a nucleon-nucleon model is directly extended to nucleus-nucleus collisions without examining proton-nucleus collisions. Our opinion is that a model for nuclear collisions should first be examined for NA collisions and then extended to AB collisions.

The notion of constituent quarks as the units of collision has been shown to be very useful to describe not only hadron-hadron collisions but also hadron-nucleus (hA) collisions at high energies. In particular, successful results have been obtained in application to the projectile fragmentation region of hA collisions, since the first application to hA collisions by Anisovich *et al.* [12] and, later on, further developed by several authors [13–17]. General reviews on the constituent quark model have recently been given by Bjorken [18].

In this paper, we first formulate the CQM relevant to nucleon-nucleon, nucleon-nucleus, and nucleus-nucleus collision dynamics at high energy by considering quarks, the constituents of hadrons, as the unit of collision instead of hadrons. When the projectile nucleon is incident on the target in nucleon-nucleon collisions, the collided nucleon has the probability of becoming three types of wounded nucleon with one, two, or all of the three interacted quarks. In the case of nucleon-nucleus collision, the incident nucleon after collision has these probabilities by multiple collision with individual nucleons within the target nucleus. In nucleus-nucleus collisions, each collided nucleon from the projectile nucleus becomes one of the three types of wounded nucleons. This distinction of the three types of wounded nucleons is a crucial difference from multiple-collision models constructed at the nucleon level. The three probabilities of quark absorption can be calculated from the given nuclear density and the total inelastic quark-quark cross section $\sigma_{\text{inel}}^{qq}$.

The three probabilities are used to estimate the degree of nuclear stopping or the rapidity distribution in high energy nucleus-nucleus collisions. The rapidity density distribution or the momentum distribution in nuclear collisions is expressed by three factors: the flavor factor, the quark interaction probability of the incident nucleon, and the fragmentation function. The flavor factor is introduced to make a distinction of whether a final state baryon is an observed

proton, a neutron, or a nucleon decayed from a hyperon. The determination of fragmentation function $f_i(x)$ comes from fitting the data on proton-proton [19] and proton-nucleus collision [20].

This paper is organized as follows. In Sec. II, we show the assumption of CQM and the quark interaction probabilities having three types of wounded nucleons with one, two, or all the three interacted quarks in nucleon-nucleon collisions at high energy. In Sec. III, the quark interaction probabilities in nucleon-nucleus collisions are given as a function of the mass number A in nucleon-nucleus collision. In Sec. IV, the average numbers of three types of wounded nucleons are calculated for AA interaction. In Sec. V, we compute the fractional momentum distribution of protons in pA collision. In Sec. VI, we calculate the rapidity distribution of leading protons in AA interaction. Finally, Sec. VII is devoted to conclusions and discussions.

II. QUARK INTERACTIONS IN NUCLEON-NUCLEON COLLISION

We start by giving the outline of the assumptions of the CQM pertinent to the description of nuclear stopping in high energy nuclear collisions. The CQM is based on three fundamental assumptions that are related to the structure of hadrons, the interactions between constituents of the projectile and the target hadrons, and the hadronization of quarks in participant nucleons [12–17]. We first assume that a hadron (meson or baryon) consists of two or three spatially separated constituent quarks. Secondly, in a hadron-hadron, hadron-nucleus, or nucleus-nucleus collision, some quarks from the projectile are assumed to interact independently with some quarks from the target, thus losing a considerable fraction of their initial momenta, while the quarks that escape from colliding in both the projectile and the target pass through retaining their initial momenta. The third assumption claims that those quarks hadronize eventually via fragmentation and recombination mechanism.

In order to calculate the total inelastic cross section for nucleon-nucleon collisions in terms of CQM, we need the probability of having a quark-quark inelastic collision when one quark in the projectile is at an impact parameter $\boldsymbol{b}$ relative to another quark in the target, which is given by

$$h(\boldsymbol{b})=\sigma_{\rm inel}^{qq}\delta^{(2)}(\boldsymbol{b}) \tag{1}$$

in the point particle approximation. The integration over impact parameter gives the total inelastic cross section of quark-quark collisions:

$$\int h(\boldsymbol{b})d\boldsymbol{b}=\sigma_{\rm inel}^{qq}. \tag{2}$$

We consider the collision of a beam nucleon N with a target nucleon N'. To the probability of a quark-quark collision (1), by multiplying the probability elements for finding a quark $\rho_N(\boldsymbol{b}_N)d\boldsymbol{b}_N dz_N$ and $\rho_{N'}(\boldsymbol{b}_{N'})d\boldsymbol{b}_{N'}dz_{N'}$ in the volume element $d\boldsymbol{b}_N dz_N$ and $d\boldsymbol{b}_{N'}dz_{N'}$, and by integrating over the collision axis z_N and $z_{N'}$, we obtain the probability that a particular quark in N interacts with a particular quark in N' when N and N' are at an impact parameter $\boldsymbol{b}$ relative to each other,

$$W(\boldsymbol{b})=\int d\boldsymbol{b}_N d\boldsymbol{b}_{N'}\rho_N(\boldsymbol{b}_N)\rho_{N'}(\boldsymbol{b}_{N'})h(\boldsymbol{b}-\boldsymbol{b}_N+\boldsymbol{b}_{N'}), \tag{3}$$

where $\rho_N(\boldsymbol{b}_N)$ is the z_N-integrated normalized quark distribution in the nucleon:

$$\rho_N(\boldsymbol{b}_N)=\int \rho_N(\boldsymbol{b}_N,z_N)dz_N. \tag{4}$$

It is normalized as

$$\int \rho_N(\boldsymbol{b}_N)d\boldsymbol{b}_N=1. \tag{5}$$

Using $W(\boldsymbol{b})$ of Eq. (3), we can evaluate the total inelastic cross section and various probabilities. When a projectile nucleon is at an impact parameter $\boldsymbol{b}$ relative to a target nucleon, the probability of the occurrence of an inelastic event is

$$g(\boldsymbol{b})=1-\{1-W(\boldsymbol{b})\}^9, \tag{6}$$

where the second term means the probability that all quarks in the projectile pass through the target nucleon without any inelastic collision. Therefore, we obtain the total inelastic cross section $\sigma_{\rm inel}^{NN'}$ for the NN' collision

$$\sigma_{\rm inel}^{NN'}=\int d\boldsymbol{b}g(\boldsymbol{b}). \tag{7}$$

The probability $g(\boldsymbol{b})$ of Eq. (6) can also be expressed as a sum of $g^{(i)}(\boldsymbol{b})$, which is the probability that i quarks in the projectile nucleon N collide with any quarks of the target nucleon N':

$$g(\boldsymbol{b})=\sum_{i=1}^{3} g^{(i)}(\boldsymbol{b}), \tag{8}$$

where

$$g^{(i)}(\boldsymbol{b})=\binom{3}{i}[1-\{1-W(\boldsymbol{b})\}^3]^i[1-W(\boldsymbol{b})]^{3(3-i)}. \tag{9}$$

Here $\binom{3}{i}$ is the combinatorial factor and the term $1-\{1-W(\boldsymbol{b})\}^3$ implies the probability that a particular quark out of the projectile nucleon interact at least once with the quarks in the target nucleon. Integrating over the impact parameter $\boldsymbol{b}$ and dividing by the total inelastic cross section, we obtain three integrated probabilities that i quarks out of three are absorbed in nucleon-nucleon collision:

$$P_{NN'}^{(i)}=\frac{1}{\sigma_{\rm inel}^{NN'}}\int d\boldsymbol{b}g^{(i)}(\boldsymbol{b}), \tag{10}$$

which is illustrated in Fig. 1.

Given the quark density distribution $\rho_N(\boldsymbol{b})$ and the inelastic quark-quark cross section $\sigma_{\rm inel}^{qq}$, we can calculate the total inelastic proton-proton cross section $\sigma_{\rm inel}^{pp}$ and the probability of quark absorption $P_{pp}^{(i)}$ in the proton-proton collision. The quark distribution is assumed to be Gaussian for simplicity,

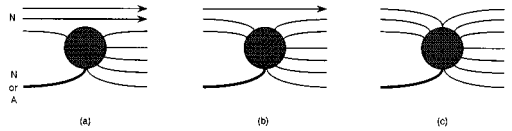

FIG. 1. Three possible interactions of the incident nucleon colliding with the target nucleon, or nucleus, in CQM. One (a), two (b), and all three (c) incident quarks interact with the target.

$$\rho_N(\boldsymbol{b})=\frac{1}{2\pi\beta^2}\exp\left(-\frac{\boldsymbol{b}^2}{2\beta^2}\right), \tag{11}$$

where the parameter β is related to the root-mean-square radius of the proton $r^p_{\rm rms}$,

$$\beta^2=\frac{1}{3}(r^p_{\rm rms})^2. \tag{12}$$

Electron scattering data [21] gives $r^p_{\rm rms}=0.862$ fm. For the inelastic quark-quark cross section as the input, we take $\sigma^{qq}_{\rm inel}=4.32$ mb in order to reproduce the total inelastic cross section of the pp collision $\sigma^{pp}_{\rm inel}=30$ mb which is observed for center-of-mass energy 3 GeV$\lesssim\sqrt{s}\lesssim$100 GeV and $\sigma^{qq}_{\rm inel}=6.64$ mb to give $\sigma^{pp}_{\rm inel}=41$ mb for $\sqrt{s}=200$ GeV [22]. The numerical values of the probability of quark interaction in pp collision for $\sigma^{qq}_{\rm inel}=4.32$ mb are shown in Table I. It should be noted that $P^{(2)}_{pp}$ is considerably large implying violation of the additive quark approximation [23].

III. QUARK INTERACTIONS IN NUCLEON-NUCLEUS COLLISION

When an incident nucleon collides with the target nucleus, the projectile nucleon can interact with many nucleons in the nucleus. We use the probabilities of quark absorption in NN collision to obtain those in NA interactions. When a nucleon is incident at an impact parameter $\boldsymbol{b}$ relative to the nucleus A, the probability for the nucleon to collide with a particular nucleon in the target nucleus is given by

$$V_A(\boldsymbol{b})=\int d\boldsymbol{b}_A\rho_A(\boldsymbol{b}_A)g(\boldsymbol{b}-\boldsymbol{b}_A), \tag{13}$$

where $\rho_A(\boldsymbol{b}_A)$ is the z-integrated nucleon density distribution of nucleus A, $d\boldsymbol{b}_A\rho_A(\boldsymbol{b}_A)$ is the z-integrated probability element of finding the nucleon, and $g(\boldsymbol{b}-\boldsymbol{b}_A)$ is the probability of inelastic NN interactions at impact parameter $\boldsymbol{b}-\boldsymbol{b}_A$ given by Eq. (6).

The total inelastic cross section for NA collisions is given by

$$\sigma^{NA}_{\rm inel}=\int d\boldsymbol{b}[1-\{1-V_A(\boldsymbol{b})\}^A]. \tag{14}$$

As $g(\boldsymbol{b}-\boldsymbol{b}_A)$ in Eq. (13) is given by Eq. (8), $V_A(\boldsymbol{b})$ is decomposed into a sum of three terms:

$$V_A(\boldsymbol{b})=\sum_{i=1}^{3}V^{(i)}_A(\boldsymbol{b}), \tag{15}$$

where $V^{(i)}_A(\boldsymbol{b})$ is the probability that i quarks in the projectile nucleon interact with a nucleon in the target nucleus,

$$V^{(i)}_A(\boldsymbol{b})=\int d\boldsymbol{b}_A\rho_A(\boldsymbol{b}_A)g^{(i)}(\boldsymbol{b}-\boldsymbol{b}_A). \tag{16}$$

Let us calculate the probabilities $P^{(j)}_{NA}$ for projectile nucleon having j interacted quarks in NA collisions. We first expand $\sigma^{NA}_{\rm inel}$ of Eq. (14) into a sum of the contributions from n $N-N$ collisions:

$$\sigma^{NA}_{\rm inel}=\sum_{n=1}^{A}\int d\boldsymbol{b}\binom{A}{n}[V_A(\boldsymbol{b})]^n[1-V_A(\boldsymbol{b})]^{A-n}. \tag{17}$$

By substituting Eq. (15) for Eq. (17) and expanding the latter, we obtain

$$P^{(j)}_{NA}=\frac{1}{\sigma^{NA}_{\rm inel}}\sum_{n=1}^{A}\binom{A}{n}\int d\boldsymbol{b}U^{(j)}_{NA}(n;\boldsymbol{b})\{1-V_A(\boldsymbol{b})\}^{A-n}, \tag{18}$$

where $U^{(j)}_{NA}(n;\boldsymbol{b})$ is the probability of having j interacted quarks in n $N-N$ collisions and is given by

$$U^{(1)}_{NA}(n;\boldsymbol{b})=U^{(1)}_{(1)}(n;\boldsymbol{b}), \tag{19a}$$

TABLE I. Comparison of a calculated total inelastic cross section $\sigma^{pA}_{\rm inel}$ with the experimental values from Ref. [20] and [26], the probabilities $P^{(i)}_{pA}$ having one, two, or all three interacted quarks in pA collisions and their average value $\langle i\rangle$.

A	$\sigma^{pA}_{\rm inel}\vert_{\rm cal}$(mb)	$\sigma^{pA}_{\rm inel}\vert_{\rm exp}$(mb)	$P^{(1)}_{pA}$	$P^{(2)}_{pA}$	$P^{(3)}_{pA}$	$\langle i\rangle$
p	30	31.3±1.2	0.81	0.17	0.02	1.21
^{9}Be	188	176±2	0.61	0.30	0.09	1.48
^{32}S	493		0.47	0.34	0.19	1.72
^{64}Cu	785	767±8	0.39	0.34	0.27	1.88
^{108}Ag	1118	1097±12	0.33	0.33	0.34	2.01
^{189}W	1584	1540±16	0.27	0.31	0.42	2.15
^{208}Pb	1724	1752±53	0.26	0.30	0.44	2.18
^{238}U	1880	1860±20	0.25	0.29	0.46	2.21

$$U_{NA}^{(2)}(n;\boldsymbol{b}) = U_{(1)}^{(2)}(n;\boldsymbol{b}) + U_{(2)}^{(2)}(n;\boldsymbol{b}) + \sum_{k=1}^{n-1} \binom{n}{k} \left[\frac{2}{3} U_{(1)}^{(1)}(k;\boldsymbol{b}) U_{(2)}^{(2)}(n-k;\boldsymbol{b}) + \frac{1}{3} U_{(1)}^{(2)}(k;\boldsymbol{b}) U_{(2)}^{(2)}(n-k;\boldsymbol{b}) \right], \quad (19b)$$

$$U_{NA}^{(3)}(n;\boldsymbol{b}) = [V_A(\boldsymbol{b})]^n - U_{NA}^{(1)}(n;\boldsymbol{b}) - U_{NA}^{(2)}(n;\boldsymbol{b}), \quad (19c)$$

where $U_{(i)}^{(j)}(n;\boldsymbol{b})$ is the probability of having j interacted quarks in n $N-N$ collisions while having i interacted quarks in each collision, and is given by

$$U_{(1)}^{(1)}(n;\boldsymbol{b}) = 3\left[\frac{1}{3} V_A^{(1)}(\boldsymbol{b})\right]^n, \quad (20a)$$

$$U_{(1)}^{(2)}(n;\boldsymbol{b}) = 3(2^n - 2)\left[\frac{1}{3} V_A^{(1)}(\boldsymbol{b})\right]^n, \quad (20b)$$

$$U_{(2)}^{(2)}(n;\boldsymbol{b}) = 3\left[\frac{1}{3} V_A^{(2)}(\boldsymbol{b})\right]^n. \quad (20c)$$

In Appendix A we present the details of our calculation of $P_{NA}^{(j)}$.

Now we need to fix the nucleon density distribution $\rho_A(\boldsymbol{b})$ in order to carry out the numerical calculation. We use the Woods-Saxon parametrization,

$$\rho_A(\boldsymbol{r}) = \frac{\rho_0}{1 + \exp(-R/a)} \quad (21)$$

for heavy nuclei ($A \geqslant 16$) while the Gaussian distribution

$$\rho_A(r) = \frac{1}{(2\pi\beta^2)^{3/2}} \exp\left(-\frac{r^2}{2\beta^2}\right) \quad (22)$$

for ^{9}Be, where both distributions are normalized as

$$\int d^3r \rho_A(r) = 1. \quad (23)$$

The parameters for each distribution can be obtained from the data on elastic electron and hadron scattering on nuclei. For the Woods-Saxon distribution, we use the parameter R and a in Ref. [24]:

$$R = 1.12A^{1/3} - 0.86A^{-1/3}, \quad a = 0.54 \text{ fm} \quad (24)$$

for ($A \geqslant 16$). For the Gaussian distribution, we take [25]

$$\beta^2 = \frac{1}{3}(r_{\text{rms}}^A)^2, \quad r_{\text{rms}}^{\text{Be}} = 2.3 \text{ fm} \quad (25)$$

for ^{9}Be. The calculated values of the total inelastic cross section $\sigma_{\text{inel}}^{pA}$ and the probabilities $P_{pA}^{(1)}$, $P_{pA}^{(2)}$, and $P_{pA}^{(3)}$ are shown in Table I and the behavior of $P_{pA}^{(i)}$ as a function of A is shown in Fig. 2. The calculated cross sections are in good agreement with the experimental values [20,26]. The process of one quark interaction with the probability $P_{pA}^{(1)}$ is dominant for light nuclei. However, even for Be, the probability of having two interacting quarks is not so small. All three probabilities have comparable magnitudes for $A \gtrsim 60$.

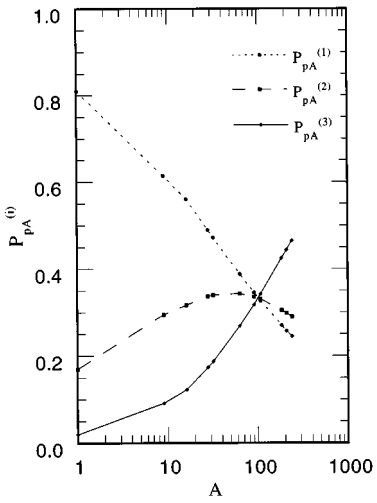

FIG. 2. The A dependence of the probabilities that one, two, or three quarks in an incident nucleon interact in pA collision.

IV. QUARK INTERACTIONS IN NUCLEUS-NUCLEUS COLLISIONS

In nucleus-nucleus collisions, many nucleons of the projectile nucleus (A) may collide with many nucleons in the target nucleus (B) by multiple collisions. After the full process of multiple collisions, the incident nucleons are divided into four types of nucleons having zero, one, two, or all the three interacted quarks. When the beam nucleus A and the target nucleus B are situated at an impact parameter $\boldsymbol{b}$ relative to each other, the probability for the occurrence of a collision between one nucleon in A and one nucleon in B is given by

$$V_{AB}(\boldsymbol{b}) = \int d\boldsymbol{b}_A d\boldsymbol{b}_B \rho_A(\boldsymbol{b}_A) \rho_B(\boldsymbol{b}_B) g(\boldsymbol{b} + \boldsymbol{b}_A - \boldsymbol{b}_B), \quad (26)$$

where $g(\boldsymbol{b})$ is given by Eq. (6).

The total inelastic cross section for AB collision is given by

$$\sigma_{\text{inel}}^{AB} = \int d\boldsymbol{b}[1 - \{1 - V_{AB}(\boldsymbol{b})\}^{AB}]. \quad (27)$$

In the same way as in Eqs. (15) and (16), the probability $V_{AB}(\boldsymbol{b})$ can be expressed as a sum of three probabilities of incident nucleons having i interacted quarks

$$V_{AB}(\boldsymbol{b}) = \sum_{i=1}^{3} V_{AB}^{(i)}(\boldsymbol{b}), \quad (28)$$

where

$$V_{AB}^{(i)}(\boldsymbol{b}) = \int d\boldsymbol{b}_A d\boldsymbol{b}_B \rho_A(\boldsymbol{b}_A) \rho_B(\boldsymbol{b}_B) g^{(i)}(\boldsymbol{b} + \boldsymbol{b}_A - \boldsymbol{b}_B), \quad (29)$$

TABLE II. Comparison of a calculated total inelastic cross section $\sigma_{\rm inel}^{AA}$ with the experimental values from Ref. [4] and empirical formula, the average number of wounded nucleons $\langle m\rangle$ and the average values for three types of wounded nucleon $\langle m_1\rangle$, $\langle m_2\rangle$, $\langle m_3\rangle$ for different triggers in AA collisions. Here ''no-bias'' implies that the impact parameter integration is carried out from zero to infinity.

$AA[\sqrt{s}(A$ Gev)]	Trigger	$\sigma_{\rm inel}^{AA}\vert_{\rm cal}$(mb)	$\sigma_{\rm inel}^{AA}\vert_{\rm exp}$(mb)	$\langle m\rangle$	$\langle m_1\rangle$	$\langle m_2\rangle$	$\langle m_3\rangle$
S+S(19.4)	No-bias	2173	1700(1740)[a]	9.4	5.6	2.9	0.9
	Veto(2%)	43	34	27.2	9.8	11.1	6.3
	E_T(11%)	239	190	25.3	10.6	9.9	4.8
	Peripheral	1422	1000	4.0	3.1	0.8	0.1
Pb+Pb(17.4)	No-bias	7660	7630[a]	77.0	32.7	26.6	17.8
	Cent.(15%)	1149	−	196.0	39.5	75.5	81.0
Au+Au(200)	No-bias	7414(7179)[b]	7325[a]	80.2	25.8	25.8	28.6
	Cent.(15%)	1112	−	192.7	18.2	54.0	120.5

[a]Values of empirical formula in Ref. [27], see text.
[b]Value for $\sigma_{\rm inel}^{qq}=4.32$ mb.

with $g^{(i)}(\boldsymbol{b}+\boldsymbol{b}_A-\boldsymbol{b}_B)$ being given by Eq. (9). The expansion of the total inelastic cross section (27) gives the probabilities of having m wounded nucleons on the beam side

$$P_{AB}(m)=\frac{1}{\sigma_{\rm inel}^{AB}}\int d\boldsymbol{b}\binom{A}{m}[1-\{1-V_{AB}(\boldsymbol{b})\}^A]^m \times[1-V_{AB}(\boldsymbol{b})]^{B(A-m)}, \tag{30}$$

and the average number is

$$\langle m\rangle=\sum_{m=1}^{A} mP_{AB}(m). \tag{31}$$

The number m is a sum of m_i, the number of nucleons having i interacted quarks:

$$m=\sum_{i=1}^{3} m_i. \tag{32}$$

We shall evaluate the probability $P_{AB}(m;m_1,m_2,m_3)$ of having such a configuration of wounded nucleons. It is convenient to introduce the probability $R_{AB}^{(j)}(\boldsymbol{b})$ that one of incident nucleons has j interacted quarks at a fixed impact parameter $\boldsymbol{b}$. It is obtained in a similar way as in NA collision by expanding the factor $1-\{1-V_{AB}(\boldsymbol{b})\}^A$. The result is

$$R_{AB}^{(j)}(\boldsymbol{b})=\sum_{n=1}^{B}\binom{B}{n}U_{AB}^{(j)}(n;\boldsymbol{b})[1-V_{AB}(\boldsymbol{b})\}]^{B-n} \tag{33}$$

with

$$\sum_{j=1}^{3} R_{AB}^{(j)}(\boldsymbol{b})=1-\{1-V_{AB}(\boldsymbol{b})\}^B. \tag{34}$$

Here, $U_{AB}^{(j)}(n;\boldsymbol{b})$ is obtained by substituting $V_{AB}^{(i)}(\boldsymbol{b})$ in AB interaction instead of $V_A^{(i)}(\boldsymbol{b})$ in NA interaction in Eqs. (19) and (20). Using the polynomial expansion, we have

$$P_{AB}(m;m_1,m_2,m_3)=\frac{1}{\sigma_{\rm inel}^{AB}}\int d\boldsymbol{b}\binom{A}{m}\binom{m}{m_1}\binom{m-m_1}{m_2} \times[R_{AB}^{(1)}(\boldsymbol{b})]^{m_1}[R_{AB}^{(2)}(\boldsymbol{b})]^{m_2}[R_{AB}^{(3)}(\boldsymbol{b})]^{m_3} \times[\{1-V_{AB}(\boldsymbol{b})\}^B]^{A-m}, \tag{35}$$

where $m_3=m-m_1-m_2$. The average number of m_j is given by

$$\langle m_j\rangle=\sum_{m=1}^{A}\sum_{m_1=0}^{m}\sum_{m_2=0}^{m-m_1} m_jP_{AB}(m;m_1,m_2,m_3). \tag{36}$$

Using the nucleon density distribution of Eq. (21) with Eq. (24), the nucleus-nucleus inelastic cross section and the average number of wounded nucleons are calculated for ^{32}S+ ^{32}S ($E_{\rm lab}=200A$ GeV), ^{208}Pb+ ^{208}Pb ($E_{\rm lab}=160A$ GeV), and ^{197}Au+ ^{197}Au ($\sqrt{s}=200A$ GeV) reactions as there are recent experimental data from CERN SPS for the first two reactions. The third reaction is chosen to give a prediction for RHIC experiment. Along with $\sigma_{\rm inel}^{AA}$, the calculated values of $\langle m\rangle$, $\langle m_1\rangle$, $\langle m_2\rangle$, and $\langle m_3\rangle$ for no-bias events are listed in Table II. For Au+Au and Pb+Pb reactions, we have shown the values estimated from the empirical formula $\sigma_{\rm inel}^{AB}=\pi r_0^2(A^{1/3}+B^{1/3}-b)^2$ with parameters $r_0=1.48$ fm and $b=1.32$ fm [27]. The calculated cross section $\sigma_{\rm inel}^{AA}$ is larger than the experimental values for S+S, while it is in good agreement with data for Au+Au and Pb+Pb reactions. The discrepancy of the cross section in S+S does not affect $P_{AB}(m;m_1,m_2,m_3)$ and $\langle m_j\rangle$.

The probability distributions $P_{AB}(m)$ of Eq. (30) and the corresponding average values $\langle m\rangle$ for S+S and Pb+Pb reactions for different triggers are shown, respectively, in Fig. 3 and Table II where the values of $\langle m_j\rangle$ are shown also. Here, veto and E_T triggers in S+S reactions mean central triggers that correspond to 2% and 11% of total inelastic cross section, respectively [4]. Corresponding to these triggers, we introduce the impact parameter cutoff $b_{\rm max}$ in our theoretical calculations so that the partial cross section

$$\int_{|\boldsymbol{b}|<b_{\rm max}} d\boldsymbol{b}\sigma_{\rm inel}^{AB}(\boldsymbol{b}) \tag{37}$$

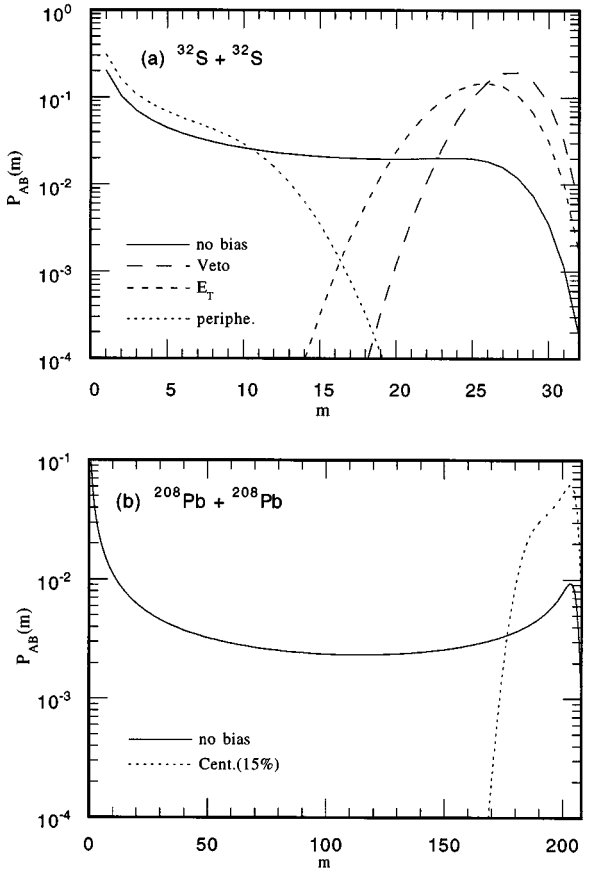

FIG. 3. The probability distribution $P_{AB}(m)$ of having m wounded nucleons for different triggers in (a) ^{32}S+^{32}S and (b) ^{208}Pb+^{208}Pb. Here we have used $\sigma_{\rm inel}^{qq}=4.32$ mb.

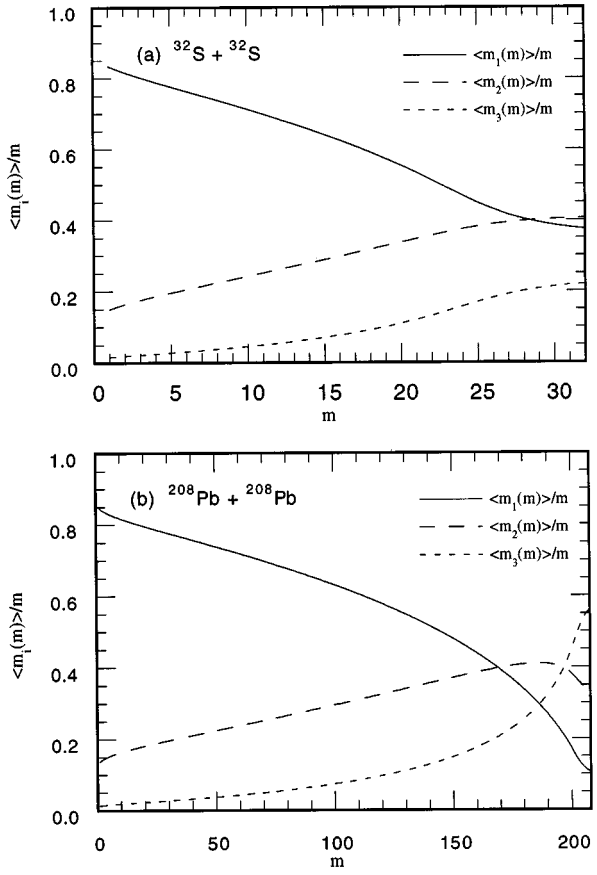

FIG. 4. The proportion of three types of wounded nucleons m_j to total wounded nucleons m in no-bias event of (a) ^{32}S+^{32}S and (b) ^{208}Pb+^{208}Pb collisions.

becomes 2% or 11% of the total cross section. The cutoff is found to be $b_{\rm max}=1.18$ fm for the veto trigger and $b_{\rm max}=2.78$ fm for the E_T trigger. For both Pb+Pb and Au+Au reactions, we take $b_{\rm max}=6.05$ fm and $b_{\rm max}=5.86$ fm, respectively, corresponding to 15% of $\sigma_{\rm inel}^{AA}$. On the other hand, the peripheral trigger in S+S reactions corresponds to 65% of $\sigma_{\rm inel}^{AA}$ which leads to the small $|\boldsymbol{b}|$ cutoff $b_{\rm min}=4.9$ fm.

In Fig. 3(a), the distribution $P_{AB}(m)$ for no-bias events of S+S reactions shows the well-known horseback shape. It is obvious that the distribution at small m is dominated by peripheral collisions while the one at large m is dominated by the central ones. The clear separation of two components in the m distribution is a consequence of the strong correlation between m and $\boldsymbol{b}$. As shown in Fig. 3(b), in Pb+Pb collisions, the distribution for no-bias events shows prominent peaks in both the smallest and the largest m region. The largest m region is of course dominated by the central collisions. The most remarkable features of the corresponding average value $\langle m\rangle$ shown in Table II is that more than 94% of the incident nucleons are wounded in the central collisions of both Pb+Pb and Au+Au.

Shown in Fig. 4 are m dependence of fractions $\langle m_i(m)\rangle/m$ in no-bias events of S+S and Pb+Pb reactions. Here $\langle m_i(m)\rangle/m$ is the average value of m_i for a fixed m. At small m, the wounded nucleon having one interacted quark m_1 dominates in both reactions. At larger m, the fractions $\langle m_1(m)\rangle/m$ and $\langle m_2(m)\rangle/m$ are comparable to each other in S+S reaction. On the other hand, for $m\gtrsim 197$, the fraction $\langle m_3(m)\rangle/m$ becomes largest in Pb+Pb reactions. For this region, $\langle m_3\rangle$ is largest in central Pb+Pb collision at $\sqrt{s}=17.4A$ GeV as seen in Table II. The trend is stronger in Au+Au collisions at RHIC energy because of larger $\sigma_{\rm inel}^{qq}$.

V. FRACTIONAL MOMENTUM DISTRIBUTIONS OF PROTONS IN PROTON-NUCLEUS COLLISIONS

In this section, we study the inclusive spectra of protons in the projectile fragmentaion region of proton-nucleus collisions, as it gives basic information on the nuclear stopping in high energy nuclear collisions. According to CQM, both participant quarks and spectator quarks hadronize via fragmentation and recombination. However, instead of giving a detailed description of such hadronization dynamics, we here introduce a phenomenological fragmentation function $f_i(x)$ $(i=1,2,3)$, which is a fractional momentum distribution of protons coming from a wounded nucleon having i interacted quarks. Assuming the independent fragmentation of each type of wounded nucleon, we express the proton spectra in pp, pA, and AB interactions as

$$\left.\frac{dN}{dx}\right|_{pp\to pX}=\sum_{i=1}^{3}\lambda_i P_{pp}^{(i)} f_i(x), \tag{38a}$$

$$\left.\frac{dN}{dx}\right|_{pA\to pX} = \sum_{i=1}^{3} \lambda_i P_{pA}^{(i)} f_i(x), \tag{38b}$$

$$\left.\frac{dN}{dx}\right|_{AB\to pX} = \sum_{i=1}^{3} \lambda_i^{(A)} \langle m_i \rangle f_i(x), \tag{38c}$$

for $0<x<1$, where dN/dx is the normalized single particle inclusive cross section $\sigma_{\text{inel}}^{-1} d\sigma/dx$ and x is the Feynman scaling variable defined in c.m. system. Moreover, λ_i and $\lambda_i^{(A)}$ are the flavor factors that can be interpreted as the probabilities of finding a proton in the hadronization product from wounded nucleon having i interacted quarks provided the effect of baryon-antibaryon pair production is negligible. The probabilities $P_{pp}^{(i)}$ and $P_{pA}^{(i)}$ are given by Eqs. (10) and (18) while $\langle m_i \rangle$ are given by Eq. (36) and all the $f_i(x)$ are normalized as

$$\int_0^1 dx f_i(x) = 1. \tag{39}$$

It is obvious that the right-hand side (RHS) of Eq. (38), being integrated over x from 0 to 1, just gives the average multiplicity of the final-state protons for each reaction in the beam fragmentation region.

Three fragmentation functions can be determined if data on three different reactions are given. In addition to $pp\to pX$ of Ref. [19], we use data on $p\text{Cu}\to pX$ and $p\text{Ag}\to pX$ provided by two experimental groups [20,28] in order to cover the wide x range. As Ref. [28] gives only the cross sections at fixed p_T's, we assume that they are proportional to the p_T-integrated cross section:

$$x\frac{d\sigma}{dx} = \kappa E \left.\frac{d\sigma}{d\boldsymbol{p}}\right|_{\text{fixed } p_T}. \tag{40}$$

Actually the constant κ can be determined by requiring that the data of Ref. [28] at $p_T = 0.3$ GeV/c coincide with the data of Ref. [20] in the range $0.3<x<0.6$ where there exist data points from both groups. Such a procedure is possible because the x dependence of a fixed-p_T cross section of [28] is really similar to $xd\sigma/dx$ of [20] as shown in Figs. 6(c) and 6(d). The values of κ are $\kappa = 1.30$ and 1.20 [$(\text{GeV}/c)^2$] for $A = \text{Cu}$ and Ag, respectively. For information, the same procedure has been applied to $pp\to pX$ with the result that $\kappa = 1.18$ [$(\text{GeV}/c)^2$]. See Fig. 6(a). It is remarkable that the values of κ are almost the same, i.e., independent of A in the three cases.

Applying data on three different reactions to Eqs. (38a) and (38b), one can determine the three fragmentaion functions. However, the immediate application gives too large uncertainties for $f_2(x)$ and $f_3(x)$ due to the propagation of the experimental errors. We accordingly assume that $f_3(x)\sim 0$ for $x\gtrsim 1/3$ because a wounded nucleon having all the three interacted quarks loses most of its incident momentum. The fragmentation functions thus obtained are shown as points with error bars in Fig. 5, where they represent the values of the fragmentation functions including the flavor factors, $F_i(x) = \lambda_i f_i(x)$ at various x.

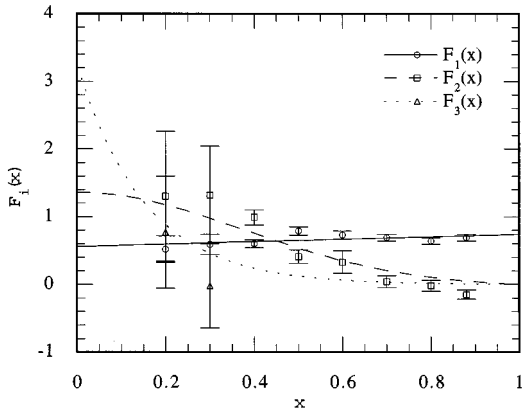

FIG. 5. The fragmentation functions $F_i(x)$ obtained from the fractional momentum distribution of protons in pp, pCu, and pAg reactions.

Though the fragmentation functions have been determined at various x, we need $F_i(x)$ for all x in order to calculate the nuclear stopping power in any reactions. In this case a meaningful χ^2 fit for the whole x region is impossible because of absence of the experimental data at $x<0.2$ and the large errors of data point at $0.2\leqslant x\leqslant 0.3$. Therefore, we assume appropriate functional forms and impose some physical conditions: $F_1(x)$ is assumed to be a linear function of x, $F_2(x)$ and $F_3(x)$ are Gaussian and exponential, repectively, with conditions on the average fractional momenta $\langle x\rangle_1 > \langle x\rangle_2 > \langle x\rangle_3$ and another condition on the flavor factors $\lambda_1 > \lambda_2 > \lambda_3$. Here, we do not use the $pp\to pX$ data point at $x>0.9$ shown in Fig. 6(a) because they are dominated by the diffractive contribution. The inequality for the average fractional momenta $\langle x\rangle_i = \int dx x f_i(x)$ means that a wounded nucleon with more interaction loses more momentum. It is obvious from pp data that $\lambda_1 \simeq 0.7$, which indicates that the probability of flavor change, is small for a single interaction. In such a case, it is reasonable to assume that the probability of flavor change increases as the number of interacted quarks increases. Therefore, λ_3 will be the smallest. However, a consideration based on a simple model indicates that it cannot be much smaller than 0.5. For example, if we consider only two flavors u and d and if the memory of the flavor of the projectile proton is completely lost in the collision with $i=3$, then a baryon made of (uud) may be formed with probability 1/2 provided only a proton and a neutron are possible final states. Thus we have assumed that $\lambda_1 \simeq 0.7 > \lambda_2 > \lambda_3 \simeq 0.5$ in the parameter fitting. The resultant fragmentation functions are

$$F_1(x) = 0.56 + 0.18x, \tag{41a}$$

$$F_2(x) = 1.4\{\exp(-3.54x^2) - \exp(-3.54)\}, \tag{41b}$$

$$F_3(x) = 3.25\exp(-6.52x). \tag{41c}$$

As shown in Fig. 5, $F_1(x)$ is nearly constant while both $F_2(x)$ and $F_3(x)$ decrease toward zero as x increases. The flavor factors are $\lambda_1 = 0.65, \lambda_2 = 0.61$, and $\lambda_3 = 0.50$ and the average fractional momenta are $\langle x\rangle_1 = 0.52$, $\langle x\rangle_2 = 0.28$, and $\langle x\rangle_3 = 0.15$. The error of λ_1 is some 10% provided the func-

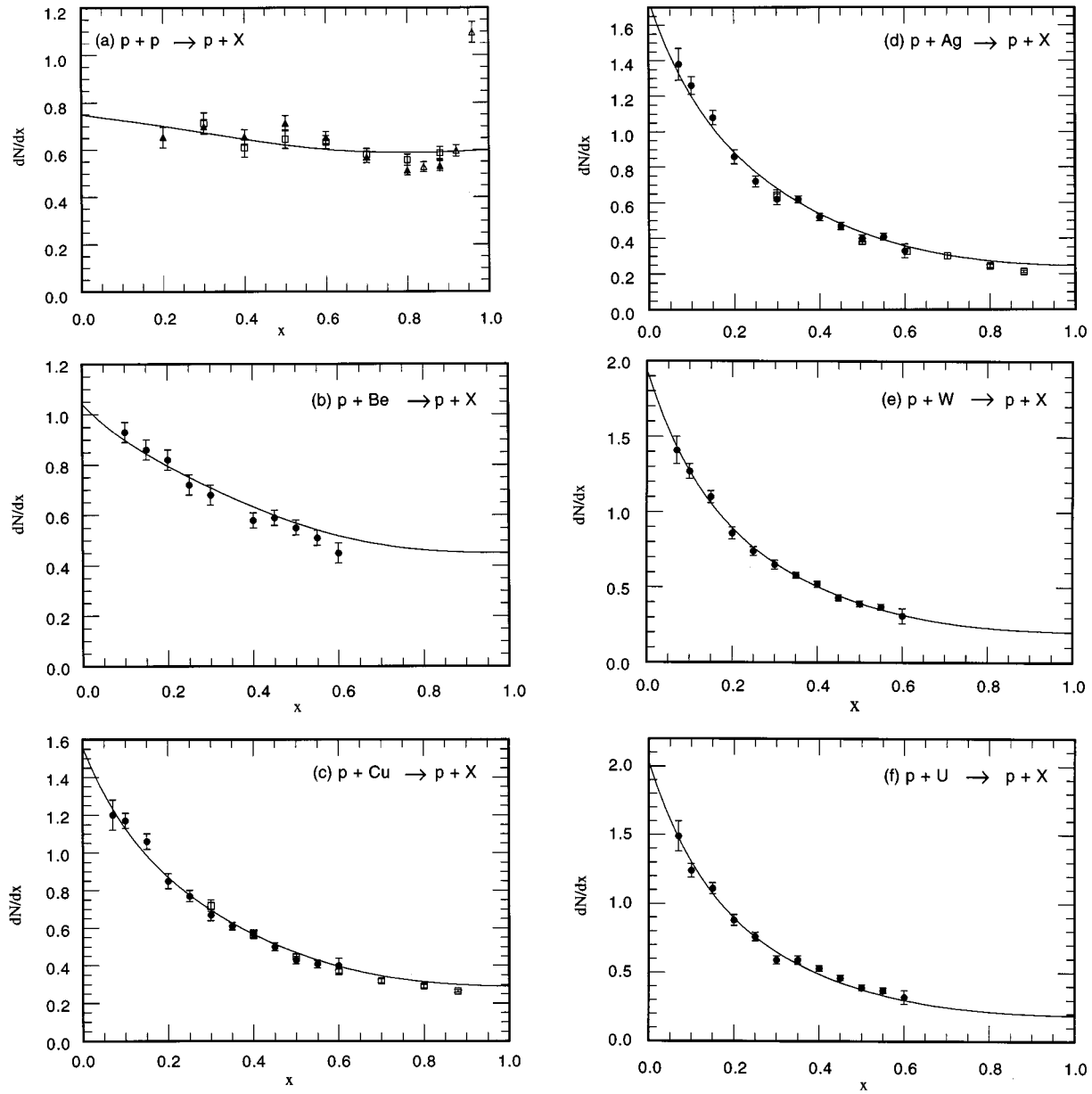

FIG. 6. The proton spectra in pA collisions for $A=p$ (a), Be (b), Cu (c), Ag (d), W (e), and U (f); pp, pCu, and pAg data are used as inputs. Curves show the model result while data points are taken from [19] (p_T-integrated pp data at 100 GeV/c; triangles), [20] (p_T-integrated pA data at 100 GeV/c; solid circles) and [28] (p_T-fixed pp and pA data at 120 GeV/c; open squares).

tional form of $F_1(x)$ is fixed. The errors of λ_2 and λ_3 cannot be estimated because the errors of data points at small x in Fig. 5 are too large.

In Fig. 6, the calculated proton spectra for $pA \rightarrow pX$ reactions ($A=p$,Be,Cu,Ag,W and U) are compared with the experimental data [19,20,28]. Our theoretical proton spectra estimated from Eq. (38) with above fragmentation functions (41) and probabilities of quark absorption given in Table I reproduce not only the input data (p,Cu,Ag) but also the other data (Be,W,U). This result suggests the validity of CQM.

TABLE III. Flavor factors $\lambda_i^{(A)}$ calculated by Eqs. (B1) and (B2) in Appendix B.

A	$\lambda_1^{(A)}$	$\lambda_2^{(A)}$	$\lambda_3^{(A)}$
S	0.415	0.415	0.415
Pb	0.365	0.374	0.397
Au	0.368	0.376	0.398

A similar analysis was done by Date *et al.* [29] using data of Ref. [28]. They assumed that $P_{pp}^{(1)}=1$, $P_{pp}^{(2)}=P_{pp}^{(3)}=0$ (quark additivity) and $F_3(x)=0$. Our analysis includes the newer data [20], which covers the small x region. We do not assume the quark additivity and also do not assume that $F_3(x)=0$ at small x. In fact, $F_3(x)$ gives a dominant contribution at small x for heavy nuclei. The fact that all the $F_i(x)$'s are estimated with reasonable accuracy from pA data makes it possible to evaluate the nuclear stopping power in AA collisions rather accurately as will be shown in the next section.

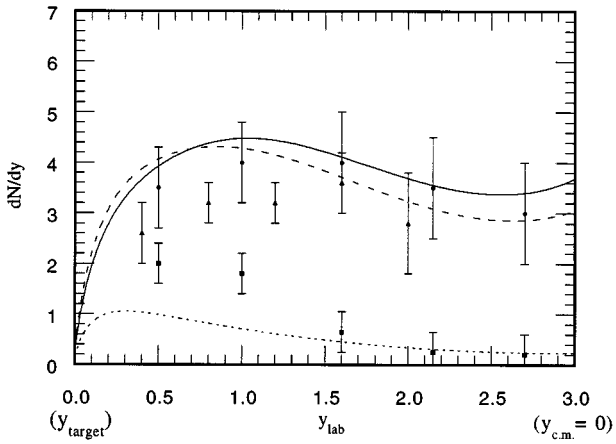

FIG. 7. The rapidity distribution of participant protons in $^{32}S+^{32}S$ collision at $E_{lab}=200A$ GeV [4]. The solid, broken, and dotted lines correspond, respectively, to veto, E_T, and peripheral triggers. The corresponding experimental data are shown by the circles, triangles, and squares, respectively.

VI. RAPIDITY DISTRIBUTION OF PROTONS IN *AA* COLLISIONS

The rapidity distributions of participant protons have recently been measured for S+S collisions at $E_{lab}=200A$ GeV by the NA35 Collaboration [4] and also for central $^{208}Pb+^{208}Pb$ collision at $E_{lab}=160A$ GeV by the NA44 Collaboration [5]. In our model the fractional momentum distribution of protons can be calculated from Eq. (38c) with $f_i(x)$ given by Eq. (41), $\langle m_i\rangle$ given in Table II, and the flavor factors $\lambda_i^{(A)}$ given in Table III. Calculation of the factors $\lambda_i^{(A)}$ is given in Appendix B. The rapidity distribution can be obtained from the fractional momentum distribution (38c) using the relation

$$\frac{dN}{dy}=\sum_{i=1}^{3}\lambda_i^{(A)}\langle m_i\rangle g_i(y), \tag{42}$$

with

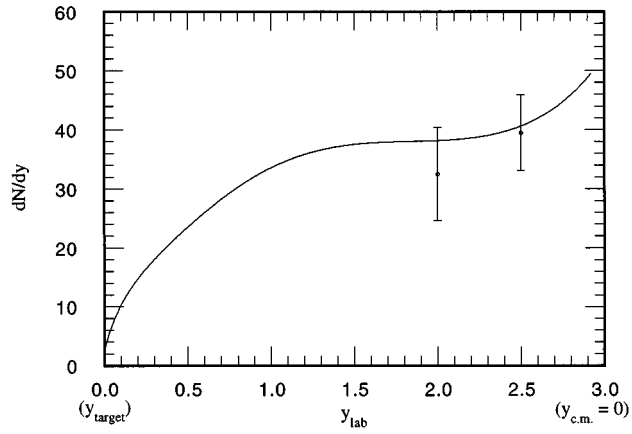

FIG. 8. The proton rapidity distribution in central (15% trigger) $^{208}Pb+^{208}$ Pb collision at $E_{lab}=160A$ GeV. The solid line stands for the theoretical result, which includes the contribution from Λ decay. Experimental data are taken from Ref. [5].

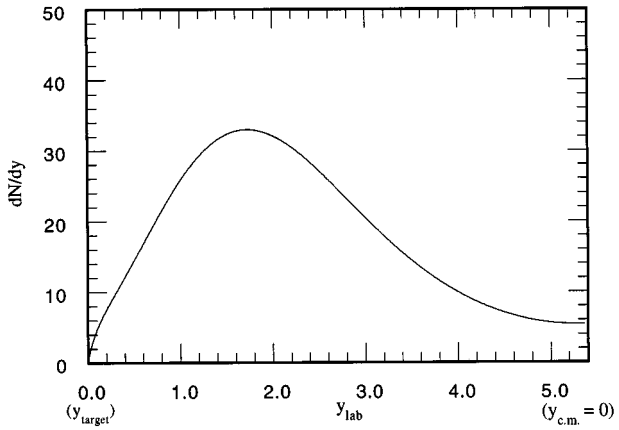

FIG. 9. Theoretical prediction for proton rapidity distribution in central (15% trigger) $^{197}Au+^{197}Au$ collision at $\sqrt{s}=200A$ GeV. Contribution from Λ decay is included. It amounts to some 20% of the total yield.

$$g_i(y)=\frac{4}{\langle p_T\rangle^2}\int_0^{p_{T\max}}dp_T p_T(2m_T\cosh y/\sqrt{s})\times f_i(2m_T\sinh y/\sqrt{s})\exp(-2p_T/\langle p_T\rangle), \tag{43}$$

where m_T is the transverse mass of the particle, $m_T{}^2=m^2+p_T^2$,

$$p_{T\max}=\sqrt{s/(4\cosh^2 y)-m^2} \tag{44}$$

and we have assumed that the x and the p_T dependences are factorized and the latter is exponential.

The results for S+S collisions are shown in Fig. 7. We have used the average values $\langle p_T\rangle = 0.622$, 0.595, and 0.45 GeV/$c$ for central (veto and E_T trigger) and peripheral collisions, respectively [4]. There is a good agreement between theoretical results and experimental data, particularly in the midrapidity region. There is a trend that the proton yield is slightly overestimated for the central triggers while it is underestimated for the peripheral collision. This may be due to a sharp cut of the impact parameter in our calculation. Our model can also reproduce well the preliminary data on central Pb+Pb collision [5] as shown in Fig. 8. Considerable yield of protons in the central rapidity region ($y_{lab}\simeq 3$) is due to the dominance of $\langle m_3(m)/m\rangle$ at the largest m. See Fig. 4(b).

In Fig. 9, the theoretical prediction is given for $^{197}Au+^{197}Au$ collisions at $\sqrt{s}=200A$ GeV to be measured at BNL-RHIC. It is remarkable that the midrapidity region becomes nearly baryon free in contrast to Pb+Pb collisions at CERN-SPS (Fig. 8).

As a useful measure of nuclear stopping power, one usually uses the mean rapidity shift of the projectile proton from their original beam rapidity $\langle\Delta y\rangle$, or the mean fractional momentum retained by the final-state proton $\langle x\rangle$ [29]. The larger the $\langle\Delta y\rangle$, the more stopping is present and hence the more baryons are produced in the central rapidity region. In Table IV, $\langle\Delta y\rangle$ and $\langle x\rangle$ and the integrated yield $\langle N_p\rangle=\int dy(dN/dy)$ calculated by our model are shown in comparison with experimental values. The rapidity shifts in S+S reactions for various triggers are in good agreement

TABLE IV. The mean multiplicities $\langle N_p \rangle$ and the mean rapidity shift $\langle \Delta y \rangle$ for $y < y_{\text{c.m.}}$ of the final state proton in our theoretical results are compared with the experimental values in Ref. [4] for S+S reaction at $E_{\text{lab}} = 200A$ GeV. $\langle x \rangle$ is the mean fractional momentum retained by the final state proton.

$AA[\sqrt{s}(A\ \text{GeV})]$	Trigger	$\langle N_p \rangle\|_{\text{exp}}$	$\langle N_p \rangle\|_{\text{cal}}$	$\langle \Delta y_p \rangle\|_{\text{exp}}$	$\langle \Delta y \rangle\|_{\text{cal}}$	$\langle x \rangle\|_{\text{cal}}$
S+S(19.4)	Veto(2%)	12.8 ± 1.4	11.3	1.58 ± 0.15	1.52	0.34
	E_T(11%)	10.3 ± 1.4	10.5	1.58 ± 0.15	1.46	0.36
	Peripheral	3.1 ± 0.8	1.7	1.00 ± 0.15	1.10	0.47
Pb+Pb(17.4)	Cent.(15%)		96.4		1.67	0.27
Au+Au(200)	Cent.(15%)		96.2		2.24	0.22

with the experimental values. The $\langle \Delta y \rangle$ in both central triggers are significantly larger than the ones in the peripheral trigger, which implies larger stopping in central collisions than in peripheral collisions. The rapidity shifts $\langle \Delta y \rangle$ in Au+Au collision at $\sqrt{s} = 200A$ GeV are much larger than that in Pb+Pb collision at 17.4A GeV, although $\langle m \rangle$ in two processes are similar to each other. This increase of $\langle \Delta y \rangle$ is due to the increase of $\langle m_3 \rangle$. In spite of the increase of $\langle \Delta y \rangle$ at RHIC energy region, the baryon number density decreases at the central rapidity region because the beam rapidity also increases. The mean fractional momentum $\langle x \rangle$ in central collisions of heavy nuclei is smaller than that in central collisions of light nuclei by about 0.1. However, still more than 20% of the incident momentum is carried by the leading nucleons in central collisions of heavy nuclei.

The mean proton multiplicity $\langle N_p \rangle$ calculated from our model for S+S collision is in good agreement with data within experimental errors. It is remarkable that $\langle N_p \rangle$ in central collisions of heavy nuclei is larger than the number of incident protons. This is due to the charge asymmetry of incident nuclei. Consider, for example, collisions of fictitious nuclei made of only neutrons.

VII. CONCLUSIONS AND DISCUSSIONS

It has been shown that our theoretical results of proton spectra are in good agreement with experimental data for both the fractional momentum distribution in pA reactions and the rapidity distributions in central $^{32}S + ^{32}S$ collision at $E_{\text{lab}} = 200A$ GeV and central $^{208}Pb + ^{208}Pb$ collision at $E_{\text{lab}} = 160A$ GeV (CERN-SPS). This result suggests strongly the validity of the constituent quark model. It is predicted that the central rapidity region in $^{197}Au + ^{197}Au$ collision at RHIC energy region will be nearly baryon-free. In general the baryon number density in the central rapidity region increases with increasing mass number of colliding nuclei, whereas it decreases with increasing incident energy. During the course of this analysis, we have established a formula, (35) for the probability of having three types of wounded nucleons in AB collisions and have determined the fragmentation functions (41) for those wounded nucleons. The probabilities given by Eqs. (10), (18), and (35), of having different quark interactions in NN, NA, and AB collisions should be useful to evaluate various spectra, e.g., the transverse energy distribution, in nuclear collisions at quark level.

It is worthwhile to compare our model with other models for nuclear stopping. For S+S reaction, the experimental data show a flat rapidity distribution of protons in agreement with our model and VENUS [7] while HIJING [11] shows stronger transparency. For Pb+Pb collision, our model and RQMD [10] predict similar strong stopping [5] contrary to VENUS and HIJING, which give weaker stopping. The different models lead to different predictions for the nuclear stopping. It should be stressed that the proton spectra of AB collisions in our model result from fitting the pp and pA data through Eq. (38). In general, any reasonable extrapolation from pp to AB via pA will give a similar result, a rather strong nuclear stopping.

Our model can describe the proton spectra in pp, pA and AB collisions in a unified manner. The notable feature of the fundamental formula (38) not shared with other models, is the factorization of x and A dependences. Equation (38) summarizes the crucial feature of our dynamical assumptions that different types of wounded nucleons distinguished by the number of interacted quarks hadronize differently and independently. One has to notice that fragmentation functions that have been determined by the experimental data in this work should be eventually derived from theoretical considerations in the future. Anyway, we would like to stress that the constituent quark model is so simple that it has only a small number of free adjustable parameters or functions: $\sigma_{\text{inel}}^{qq}$ and $f_i(x)$ for $i = 1$, 2, and 3. Although most models have recently been constructed as complicated event generators, we feel it still worthwhile to pursue a simple phenomenological model that allows an analytical calculation and a simple interpretation of the results of data analysis.

ACKNOWLEDGMENTS

The authors would like to thank S. Esumi for kind correspondence on NA44 data of lead-lead collisions (CERN). One of the authors (T.K.C.) is grateful to the Japanese Government for financial support.

APPENDIX A: THE PROBABILITIES OF HAVING j INTERACTED QUARKS IN n NUCLEON-NUCLEON COLLISIONS

In NA collisions, we have considered that the incident nucleon collides with many nucleons of the target nucleus by multiple collisions. By expanding the formula of the total inelastic cross section (14), the probabilities of having n (nucleon-nucleon) collisions in an average collision with all possible impact parameters are written as

$$P_{NA}(n) = \frac{1}{\sigma_{\text{inel}}^{NA}} \int d\boldsymbol{b} \binom{A}{n} [V_A(\boldsymbol{b})]^n [1 - V_A(\boldsymbol{b})]^{A-n}. \tag{A1}$$

To obtain the probabilities of projectile nucleon having j interacted quarks in n collisions, it is enough to expand only the second factor of Eq. (A1) $[V_A(\boldsymbol{b})]^n$, the probability of having exactly n collision, in terms of $V_A^{(i)}(\boldsymbol{b})$, the probability of finding i interacted quarks in one nucleon-nucleon collision, as follows;

$$[V_A(\boldsymbol{b})]^n=\sum_{k=0}^{n}\sum_{l=0}^{n-k}\binom{n}{k}\binom{n-k}{l}\{V_A^{(1)}(\boldsymbol{b})\}^k\{V_A^{(2)}(\boldsymbol{b})\}^l \times\{V_A^{(3)}(\boldsymbol{b})\}^{n-k-l}. \tag{A2}$$

The factor $\{V_A^{(i)}(\boldsymbol{b})\}^k$ on the RHS implies the probability of having k collision with the same $V_A^{(i)}(\boldsymbol{b})$ and can be expressed in terms of $U_{(i)}^{(j)}(k;\boldsymbol{b})$, the probabilities of having j interacted quarks in k *collisions* while having i interacted quarks in *each nucleon-nucleon collision*. For k collisions with the same probability $V_A^{(1)}(\boldsymbol{b})$, it is given by

$$\{V_A^{(1)}(\boldsymbol{b})\}^k=U_{(1)}^{(1)}(k;\boldsymbol{b})+U_{(1)}^{(2)}(k;\boldsymbol{b})+U_{(1)}^{(3)}(k;\boldsymbol{b}), \tag{A3}$$

where

$$U_{(1)}^{(1)}(k;\boldsymbol{b})=3\left[\frac{1}{3}V_A^{(1)}(\boldsymbol{b})\right]^k, \tag{A4}$$

$$U_{(1)}^{(2)}(k;\boldsymbol{b})=3(2^n-2)\left[\frac{1}{3}V_A^{(1)}(\boldsymbol{b})\right]^k, \tag{A5}$$

$$U_{(1)}^{(3)}(k;\boldsymbol{b})=\{(3^n-3)-3(2^n-2)\}\left[\frac{1}{3}V_A^{(1)}(\boldsymbol{b})\right]^k. \tag{A6}$$

Here, Eq. (A4) is the probability of one quark in the incident nucleon interacting repeatedly with any nucleon of target nucleus and then having one interacted quark in k collisions. Equation (A5) implies the probability of one quark interacting with the target nucleon, also another quark interacting in other collision, then having two interacted quarks. The probability of three quarks interacting in each collision appears in Eq. (A6). When the projectile nucleon interacts with the target nucleon simultaneously in one collision, there are two possibilities of having two interacted quarks and three interacted quarks in l collision as follows:

$$\{V_A^{(2)}(\boldsymbol{b})\}^l=U_{(2)}^{(2)}(l;\boldsymbol{b})+U_{(2)}^{(3)}(l;\boldsymbol{b}), \tag{A7}$$

where

$$U_{(2)}^{(2)}(l;\boldsymbol{b})=3\left[\frac{1}{3}V_A^{(2)}(\boldsymbol{b})\right]^l, \tag{A8}$$

$$U_{(2)}^{(3)}(l;\boldsymbol{b})=(3^n-3)\left[\frac{1}{3}V_A^{(2)}(\boldsymbol{b})\right]^l. \tag{A9}$$

In a case where all three incident quarks are participating in one $N-N$ collision, the projectile nucleon has necessarily three interacted quarks in m $N-N$ collisions:

$$\{V_A^{(3)}(\boldsymbol{b})\}^m=U_{(3)}^{(3)}(m;\boldsymbol{b}), \tag{A10}$$

Substituting Eqs. (A3), (A7), and (A10) for Eq. (A2), we obtain

$$[V_A(\boldsymbol{b})]^n=\sum_{k=0}^{n}\sum_{l=0}^{n-k}\binom{n}{k}\binom{n-k}{l}\{U_{(1)}^{(1)}(k;\boldsymbol{b})+U_{(1)}^{(2)}(k;\boldsymbol{b}) +U_{(1)}^{(3)}(k;\boldsymbol{b})\}\{U_{(2)}^{(2)}(l;\boldsymbol{b})+U_{(2)}^{(3)}(l;\boldsymbol{b})\} \times\{U_{(3)}^{(3)}(n-k-l;\boldsymbol{b})\}. \tag{A11}$$

In Eq. (A11), all terms including $j=3$ contribute the probability of having three interacted quarks in n collisions and the cross terms are divided into the probabilities of having two or three interacted quarks with suitable weight. Thus one can write $[V_A(\boldsymbol{b})]^n$ in terms of $U_{NA}^{(j)}(n;\boldsymbol{b})$, the probability of having j interacted quarks in n nucleon-nucleon collisions in the form

$$[V_A(\boldsymbol{b})]^n=U_{NA}^{(1)}(n;\boldsymbol{b})+U_{NA}^{(2)}(n;\boldsymbol{b})+U_{NA}^{(3)}(n;\boldsymbol{b}), \tag{A12}$$

where

$$U_{NA}^{(1)}(n;\boldsymbol{b})=U_{(1)}^{(1)}(n;\boldsymbol{b}), \tag{A13}$$

$$U_{NA}^{(2)}(n;\boldsymbol{b})=U_{(1)}^{(2)}(n;\boldsymbol{b})+U_{(2)}^{(2)}(n;\boldsymbol{b})+\sum_{k=1}^{n-1}\binom{n}{k} \times\left[\frac{2}{3}U_{(1)}^{(1)}(k;\boldsymbol{b})U_{(2)}^{(2)}(n-k;\boldsymbol{b}) +\frac{1}{3}U_{(1)}^{(2)}(k;\boldsymbol{b})U_{(2)}^{(2)}(n-k;\boldsymbol{b})\right], \tag{A14}$$

$$U_{NA}^{(3)}(n;\boldsymbol{b})=[V_A(\boldsymbol{b})]^n-U_{NA}^{(1)}(n;\boldsymbol{b})-U_{NA}^{(2)}(n;\boldsymbol{b}). \tag{A15}$$

From Eqs. (A12) and (A1), therefore, we obtain the formulas for the probability function of quark absorption in average n collisions.

APPENDIX B: CALCULATION OF THE FLAVOR FACTORS IN *AA* COLLISIONS

The flavor factors in AA collisions are the weighted average of the probabilities that a proton is produced from an incident proton or from an incident neutron. If one neglects the effect of baryon-antibaryon pair production and assumes that an incident nucleon fragments into either p, n, or Λ, one has

$$\lambda_i^{(A)}=\frac{Z}{A}(\lambda_i)+\left(1-\frac{Z}{A}\right)(1-\lambda_i-\eta), \tag{B1}$$

where η is the probability that an incident nucleon is converted into Λ after interaction and Z/A is the proportion of the proton over the atomic mass. For a charge symmetric system $(Z/A=1/2)$, it reduces to

$$\lambda_1^{(A)}=\lambda_2^{(A)}=\lambda_3^{(A)}=\frac{1}{2}(1-\eta). \tag{B2}$$

The numerical value of η is estimated to be 0.17 by using the experimental data on central S+S collisions [4,30].

[1] L. D. Landau, Izv. Akad. Nauk SSSR, Ser. Fiz. **17**, 51 (1953).
[2] J. D. Bjorken, Phys. Rev. D **27**, 140 (1983).
[3] J. Barrette *et al.*, Phys. Rev. Lett. **64**, 1219 (1992); **70**, 2996 (1993)
[4] J. Bächler *et al.*, Phys. Rev. Lett. **72**, 1419 (1994).
[5] S. Esumi, talk presented at the International Symposium on Quantum Interferometry Studies in High Energy Nuclear Collision, Hiroshima, Japan, 1995; Genshikaku Kenkyu **40**, 159 (1996).
[6] R. J. Glauber, in *Lectures in Theoretical Physics*, edited by W. E. Brittin and L. G. Dunham (Interscience, New York, 1959), Vol. 1, p. 315.
[7] K. Werner, Phys. Rep. **232**, 87 (1993).
[8] See for a review, C. Y. Wong, *Introduction to High-Energy Heavy-Ion Collisions* (World Scientific, Singapore, 1994).
[9] M. Gyulassy, Nucl. Phys. **A590**, 431c (1995).
[10] H. Sorge, H. Stocker, and W. Greiner, Nucl. Phys. **A498**, 567c (1989); **A566**, 633c (1994).
[11] X. N. Wang and M. Gyulassy, Phys. Rev. D **44**, 3501 (1991); **45**, 844 (1992).
[12] V. V. Anisovich, Yu. M. Shabelski, and V. M. Shekhter, Nucl. Phys. **B133**, 477 (1978).
[13] N. N. Nikolaev and S. Pokorski, Phys. Lett. **80B**, 290 (1979).
[14] A. Dar and F. Takagi, Phys. Rev. Lett. **44**, 768 (1980).
[15] A. Białas and E. Białas, Phys. Rev. D **20**, 2854 (1979).
[16] F. Takagi, Prog. Theor. Phys. **65**, 1350 (1981).
[17] F. Takagi, Phys. Rev. D **27**, 1461 (1983).
[18] J. D. Bjorken, Acta Phys. Pol. B **23**, 637 (1992); in *Proceedings of the 10th Lake Louise Winter Institute: Quarks and Colliders*, edited by A. Astbury *et al.* (World Scientific, Singapore, 1995).
[19] A. E. Brenner *et al.*, Phys. Rev. D **26**, 1497 (1982).
[20] R. Bailey *et al.*, Z. Phys. C **29**, 1 (1985).
[21] G. G. Simon *et al.*, Nucl. Phys. **A333**, 381 (1980).
[22] Particle Data Group, K. Hikasa *et al.*, Phys. Rev. D **45**, S1 (1992).
[23] A. Białas, W. Czyz, and L. Lesniak, Phys. Rev. D **25**, 2328 (1982).
[24] A. Bohr and B. R. Mottelson, *Nuclear Structure, Vol. 1: Single-Particle Motion* (Benjamin, New York, 1969).
[25] S. P. Denisov *et al.*, Nucl. Phys. **B61**, 62 (1973).
[26] A. S. Carroll *et al.*, Phys. Lett. **80B**, 319 (1979).
[27] E. O. Abdrahmanov *et al.*, Z. Phys. C **5**, 1 (1980).
[28] D. S. Barton *et al.*, Phys. Rev. D **27**, 2580 (1983).
[29] See for example, S. Daté, M. Gyulassy, and H. Sumiyoshi, Phys. Rev. D **32**, 619 (1985).
[30] J. Bartke *et al.*, Z. Phys. C **48**, 191 (1990).